

A revamped understanding of Cosmic Rays and Gamma-Ray Bursts

A. De Rújula^{a,b}

^a*Instituto de Física Teórica (UAM/CSIC), Univ. Autónoma de Madrid, Spain;*

^c*Theory Division, CERN, CH 1211 Geneva 23, Switzerland*

(Dated: December 10, 2024)

Interesting data on Gamma Ray Bursts (GRBs) and Cosmic Rays (CRs) have recently been made public. GRB221009A has a record “peak energy”. The CR electron spectrum has been measured to unprecedented high energies and exhibits a “knee” akin to the ones in all-particle or individual-element CR nuclei. IceCube has not seen high-energy neutrinos associated with GRBs. AMS has published a CR positron spectrum conducive to much speculation. We examine these data in the light of the “CannonBall Model” of GRBs and CRs, in which they are intimately related and which they do strongly validate.

PACS numbers: 98.70.Sa, 14.60.Cd, 97.60.Bw, 96.60.tk

NOTE A fraction of this paper elaborates results by S. Dado and A. Dar in [1].

I. INTRODUCTION

Concerning the Cannon Ball (CB) model a referee once said “This is almost Baron Munchausen” [2], presumably meaning a lengthy and surprising list of fabrications. But, as I shall argue, what is really surprisingly lengthy is the list of correct predictions of the model.

The CB model [3] describes long-duration gamma-ray bursts (referred in this paper simply as GRBs), X-rays flashes (XRFs), short-duration GRBs originating in neutron-star mergers [4, 5], and non-solar cosmic rays (called here simply CRs), as well as various other astrophysical phenomena. Early summaries can be found in [6], [7], the second of which will be referred to as DD2008.

Details of the model and some of its predictions are given in the Appendix. Its basic assumption is that a stripped-envelope SNIc (a Type Ic supernova event) results in the axial emission of opposite jets of one or more CBs, made of ordinary matter. The observable ones have initial Lorentz factors (LFs) $\gamma_0 \equiv \gamma(t=0)$, of $\mathcal{O}(10^3)$.

The electrons in a CB inverse-Compton scatter (ICS) photons in the parent SN “glory”. This results in a γ -ray beam of aperture $\simeq 1/\gamma_0 \ll 1$ around the CB’s direction. Viewed by an observer at an angle θ relative to the CB’s direction, the individual photons are boosted in energy by a Doppler factor $\delta_0 \equiv \delta(t=0) = 1/[\gamma_0(1-\beta \cos \theta)]$ or, to a very good approximation for $\gamma_0^2 \gg 1$ and $\theta^2 \ll 1$:

$$\delta_0 = 2\gamma_0/(1 + \gamma_0^2\theta^2). \quad (1)$$

CBs are efficient relativistic *magnetic rackets*. We assumed in DD2008 that the racket’s “strings” were the magnetic fields *inside* a CB. Here we assume that the racket is the (external) magnetic field of the CB [1]. As detailed in Section IF and the Appendix, the CB-model predictions stay put. Non-solar primary cosmic-ray nuclei and electrons are made by the “collisions” between this field and the ambient ISM matter, previously ionized by the extremely intense γ -ray radiation of the GRB

pulse that a CB made. In an “elastic” collision the maximum energy acquired by a CR (in $c=1$ units) is:

$$E_{\max} = 2\gamma_0^2 M, \quad (2)$$

with M the mass of the CR electron or nuclear isotope. Spoiler: these are the energies of the spectral “knees”.

It must be emphasized ab initio that, while the CB model of GRBs is used to extract many “prior” parameters compatible with independent observations –such as the typical properties of CBs and SN glories– the same model correctly describes nuclear CRs at all energies with only one parameter chosen to fit the data [DD2008]. The description is a *first order* one for several reasons, e.g.: the Galaxy’s magnetic fields and the details of how they “confine” CRs as a function of their momentum are not precisely known, secondary CRs slightly contaminate the spectra of the primary ones. These are some of the *next order* effects that we do not address.

A. The unresolved conundrum

How is it possible to endow a CB with a humongous LF of $\mathcal{O}(10^3)$? The energy release in a SN is of $\mathcal{O}(M_\odot/10)$, the binding energy of a neutron star. The mass of a CB implied by GRB data is of $\mathcal{O}(10^{-7}M_\odot)$. On average ~ 10 of them are made in an observed GRB. Thus the energy carried by these CBs is “only” of $\mathcal{O}(10^{-3}M_\odot)$. The typical kinetic energy of a SN’s ejecta is > 50 times larger [8]. SN explosions are not yet well understood. Deciphering how all these things happen to happen would require a mastery of transient, catastrophic, relativistic, chaotic, turbulent magneto-hydrodynamics. Not a trivial task. “Seeing is believing” proofs would be images of CBs traveling with enormous LFs. Such images do exist, see the “Superluminal Motion” entry in the Appendix.

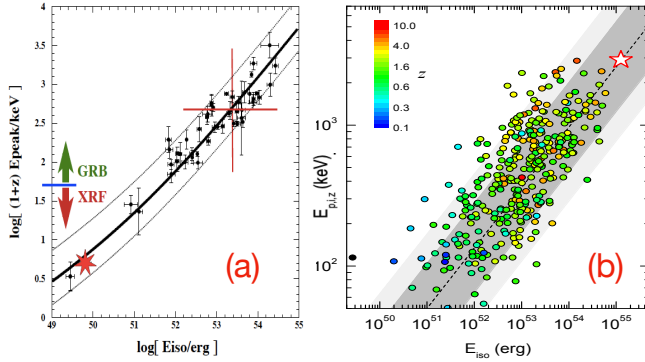


Figure 1: (a) The $[E_p, E_{iso}]$ correlation, with a slope interpolating the ones of Eqs.(5) and (6). By definition the blue line separates GRBs from XRFs. (b) Results for 315 long GRBs with known redshift observed by Konus-Wind [9]. The color of each data point represents the GRB’s redshift. Error bars are not shown. GRB221009A is indicated by a red star. The best fit Amati correlation is plotted as a dashed line.

B. An interlude on correlations

The ICS of glory photons of energy ϵ by a CB boosts their energy, as seen by an observer at redshift z , to $E_\gamma = \gamma_0 \delta_0 \epsilon / (1+z)$. Consequently, the peak energy E_p of their time-integrated energy distribution satisfies

$$(1+z) E_p \approx \gamma_0 \delta_0 \epsilon_p, \quad (3)$$

with ϵ_p the peak energy of the glory’s light, for which we choose $\epsilon_p = 1$ eV, one of the CB model’s priors [DD2008].

In the Thomson regime the nearly isotropic distribution (in the CB’s rest frame) of a number n_γ of photons is Compton scattered into an angular distribution $dn_\gamma/d\Omega \approx (n_\gamma/4\pi) \delta^2$ in the observer’s frame. Thus, the isotropic-equivalent total energy of the photons satisfies

$$E_{iso} \propto \gamma_0 \delta_0^3 \epsilon_p. \quad (4)$$

GRBs –viewed from at $\theta \sim 1/\gamma$, implying $\delta_0 \sim \gamma_0$ – satisfy

$$(1+z) E_p \propto [E_{iso}]^{1/2}, \quad (5)$$

while far off-axis ones ($\theta^2 \gg 1/\gamma_0^2$, implying $\delta_0 \propto \theta^{-2}$) may be dubbed XRFs, have a much lower E_{iso} , and satisfy

$$(1+z) E_p \propto [E_{iso}]^{1/3}. \quad (6)$$

The predicted $[E_p, E_{iso}]$ correlations [10] are shown in Fig.(1a), where a fit was made interpolating a power law from a 1/3 to a 1/2 behavior. This “Amati” correlation was later observationally discovered [11]. Some recent results [9] are shown in Fig.(1b), where the best-fit line has a slope 0.42, which happens to be the average of the slopes in Eqs.(5) and (6).

C. CB-model consequences of GRB221009A

The fact that GRB221009A, like all others, satisfies the Amati correlation is not what makes it interesting. The

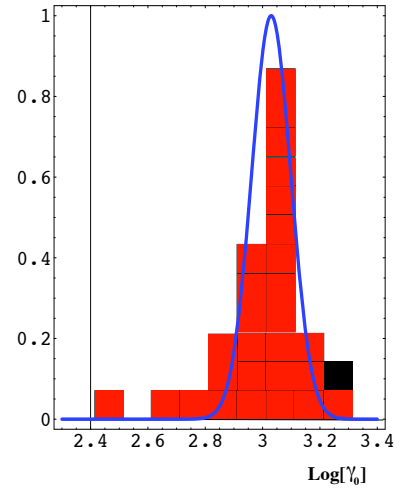


Figure 2: Distribution of CB Lorentz factors, from the analysis of their GRB afterglows and a fit to it [DD2008] and, in black, the result for GRB221009A, extracted from the peak energy of its γ rays. Low LF CBs no doubt escape detection.

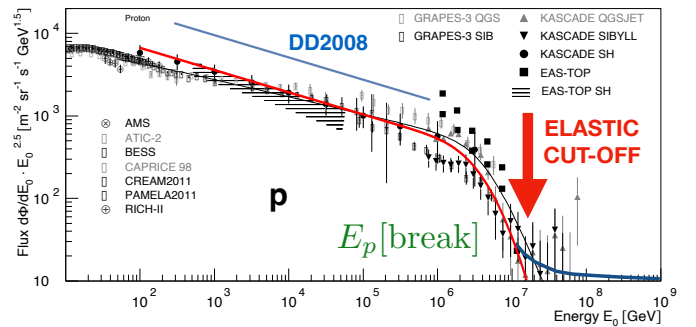


Figure 3: The p (or “H”) knee extends from $E_p \simeq 10^6$ to $\simeq 10^7$ GeV. Above the knee the “inelastic” contribution, discussed later, dominates.

implications of its measured its measured $(1+z) E_p = 3503 \pm 133$ keV, are. Being so energetic, the CB model implies that it was observed at a small angle, so that $\delta_0 \approx \gamma_0$ and Eq.(3) implies a large γ_0 [221009A] $\approx 1.87 \times 10^3$. This result is shown in black in Fig.(2), where GRB221009A is seen along with old record breakers.

A spectrum of CR protons [12] is shown in Fig.(3). The theoretical spectrum is shown in red and the specific shape of its knee reflects the fact that it has been predicted –and convoluted– with the fit γ_0 distribution shown in Fig.(2), extracted from our analyses of *GRB afterglows* (AGs) [6, 7], not from data concerning CRs.

Combine Eqs.(2) and γ_0 [221009A] $\approx 1.87 \times 10^3$ to obtain a predicted “end of the proton’s knee” at an elastic cutoff energy 1.4×10^7 GeV, shown in Fig.(3). This is the first of the a series of good news. It verifies the idea that GRBs and CRs have a common origin.

D. Criticism of the CB model

Referees rejecting articles on the CB model typically make statements such as: *The CB should swipe-up the plasma in its path, inducing a shock, compressing and deforming it in the process.* This is based on the traditional view that SN shocks –or, more recently, narrow jets produced by SNe¹– are the accelerators of CRs. The most convincing defense of this claim is the development of instabilities and shocks in numerical simulations of the collision of two plasmas. These simulations typically employ unrealistically large electron-to-ion mass ratios (e.g. 1/15) and relative Lorentz factors of the colliding plasmas much smaller than 10^3 [13]. Also, the simulations are one-dimensional, with periodic boundary conditions in the transverse directions. It is not obvious that the results would be similar in realistic simulations of CBs.

One problem with the traditional views is that they do not result in successful comparisons with the data, unless they include, for instance, acceleration by Galactic Alfvén waves and a large number of fit parameters [14].

The particular referee quoted above continued by saying: *We are given no calculation in the paper to demonstrate what the dynamics would really look like.* In DD2008 we did explicitly introduce such dynamics (Section III). The problem is that it looks so naive.

E. Naive and first-principled results

Occasionally extremely naive predictions have a success that sophisticated first-principle derivations lack. One example is the QCD-improved quark model, wherein hadrons are analogous to atoms, made of constituent quarks whose hyperfine interactions are dictated by one gluon exchange [15]. This “naive” model explained the masses of all known S-wave mesons and baryons. And it precisely and correctly predicted the masses of their then unknown charmed counterparts [16]. It took several decades for “first-principled” lattice gauge theory computations to obtain similarly precise “post-dictions” [17].

A naive result feels less naive if its predictions are abundant and successful. The CB model of CRs makes the predictions discussed here. Its comparison with the standard views on GRBs is telling, see Table III in [18].

F. Revamping the theory itself

In DD2008 we assumed that the ISM ingredients entering a CB exited it by diffusion in its inner magnetic field and that CBs are decelerated by ingurgitating a large

fraction of the ISM they intercept². The details of the process –such as the CB’s radius– disappeared from the answer for the shape of the relativistic flux, which below the knees took the analytic form:

$$\frac{dF_{\text{elast}}}{d\gamma} \propto n_A \int_1^{\gamma_0} \frac{d\bar{\gamma}}{\bar{\gamma}^{7/3}} \int_{\max[\bar{\gamma}, \gamma/(2\bar{\gamma})]}^{\min[\gamma_0, 2\bar{\gamma}\gamma]} \frac{d\gamma_{\text{co}}}{\gamma_{\text{co}}^4}, \quad (7)$$

with n_A the number densities in the ISM.

CBs may have high spin and an intense magnetic field [1], like newly-born neutron stars. In such a case it may be this *external* magnetic field that converts the ISM it encounters into CRs. If the latter exit the CB’s “magnetic domain” by diffusion (as in DD2008) Eq.(7) would result. This “revamped” version of the CB model evades the critique that magnetic fields in a CB’s trajectory deviate CRs and the CB would catch up with them [19, 20]. A tiny fraction of $\mathcal{O}(10^{-15})$ of these “first-injected” CRs are Fermi-accelerated within the CB’s magnetic domain while diffusing out of it, to result in the same flux above the knees as in DD2008, whose predictions are then unchanged by these revamped assumptions.

First-principle simulations of a rapidly moving and rotating magnetized CB encountering the ISM and producing CRs would be difficult, and welcome.

II. UNIVERSALITY OF THE CR FLUXES

For nuclear CRs, in a domain of relativistic energies below the corresponding knees for all A , the source flux of Eq.(7) is very well approximated by

$$dF_s^A/d\gamma \propto n_A \gamma^{-\beta_s}, \quad \beta_s = 13/6. \quad (8)$$

The observed spectrum should be steeper than in Eq.(8), since Galactic confinement is a species-dependent effect, traditionally simplified for nuclear CRs as a power-law modification of the source flux by a confinement-time factor $\tau \propto (Z/p)^{\beta_c}$, or, in the relativistic domain,

$$\tau \propto (Z/E)^{\beta_c} = [Z/(A m_n \gamma)]^{\beta_c}. \quad (9)$$

All in all³

$$dF^A/d\gamma \propto n_A \gamma^{-(\beta_s + \beta_c)} \quad (10)$$

In DD2008 we adopted a value $\beta_c = 0.6$ [22], resulting in $\beta_s + \beta_c \approx 2.77$, in good agreement with the individual spectra and in excellent agreement with the all-particle value 2.75, recently measured by LHAASO-KM2A [23].

² An assumption supported by the predictions for GRB afterglows.

³ An AI program may notice that we erased a factor $(Z/A)^{\beta_c}$ in Eq.(10). This is because we assume, as in DD2008, that CRs exit their birthplace area by diffusion, as they do in the Galaxy as a whole. This compensates exactly for the $(Z/A)^{\beta_c}$ factor.

¹ If jets indeed consist in successive blobs of matter –as implied, by successive GRB pulses– that would be the skeletal CB model.

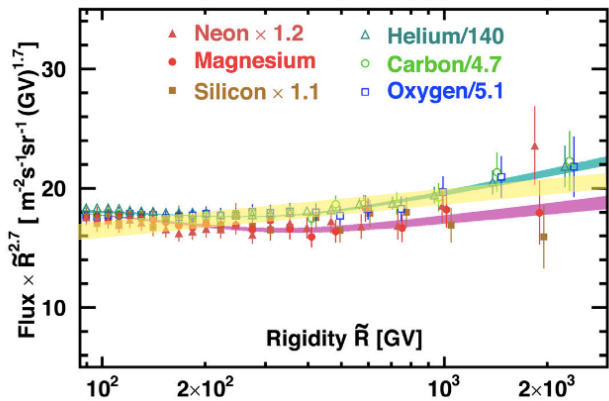


Figure 4: AMS results [21] for various primary CRs as function of rigidity. The yellow band is the result in DD2008.

It has become customary to present results on the spectra of individual CR nuclei not as functions of energy, but as functions of rigidity, $\tilde{R} \equiv p/Z$. For the relativistic nuclei in Fig.(4) $\tilde{R} \approx (A/Z) m_p \gamma$, or $\tilde{R} \propto \gamma$, since A/Z is approximately the same for all these nuclei. Thus the figure can be read as a test of Eq.(10).

One cannot say that Fig.(4) is a precise test of the *predictions* in DD2008. There we chose in τ –the CR confinement-time power law– a value of β_c [22] compatible with the data. There is no reason for τ to be so naively simple. Indeed, the Galaxy is complicated, contains spiral arms, has magnetic fields whose structure is not well known, etcetera, The observed slight hardening of the spectra at $\tilde{R} \sim 4 \times 10^2$ GV may well be due to a confinement time which is not quite a simple power law.

III. CR ELEMENTARY ABUNDANCES

We summarize here results in DD2008 because they provide a striking test of Eq.(10). In what follows we replace $\beta_s + \beta_c$ in Eq. (9) by $\beta = 2.75$, the expected and/or observed all-particle spectral index.

It is customary to present results on the composition of CRs at a fixed energy per nucleus, $E_A = 1$ TeV, as opposed to a fixed γ . Change variables ($E_A \propto A\gamma$) in Eq. (10) to obtain the prediction for the observed fluxes:

$$dF_{\text{obs}}/dE_A \propto \bar{n}_A^{\text{amb}} A^{\beta-1} E_A^{-\beta}, \quad \beta - 1 \sim 1.75, \quad (11)$$

with \bar{n}_A^{amb} the average ‘ambient’ ISM nuclear abundances –listed and discussed in detail in DD2008– in the large ‘metallicity’ environments of the SN-rich domains wherein CBs produce CRs.

At fixed energy the predictions for the CR abundances $X_{\text{CR}}(A)$ relative to protons are:

$$X_{\text{CR}}(A) \approx X_{\text{amb}}(A) A^{1.75}; \quad X_{\text{amb}}(A) \equiv \bar{n}_A^{\text{amb}}/\bar{n}_p^{\text{amb}}, \quad (12)$$

with X_{amb} the abundances, relative to H (AKA p in this context), in the mentioned domains.

The DD2008 results are shown in Fig.(5). They are remarkable, given that the input ambient abundances and

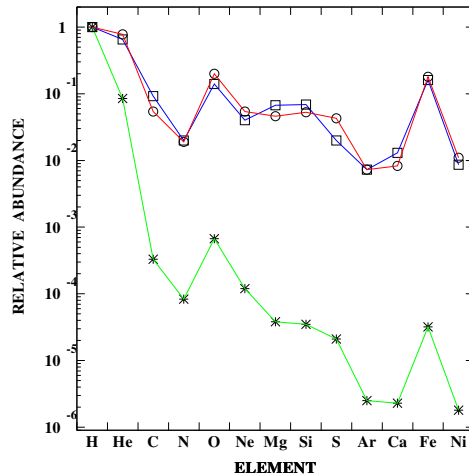


Figure 5: The relative abundances of primary CR nuclei, from H to Ni around 1 TeV [25]. The stars (joined by green lines) are solar-ISM abundances [26]. The circles (joined in red) are the predictions, with input super-bubble abundances. The squares (joined in black) are the CR observations.

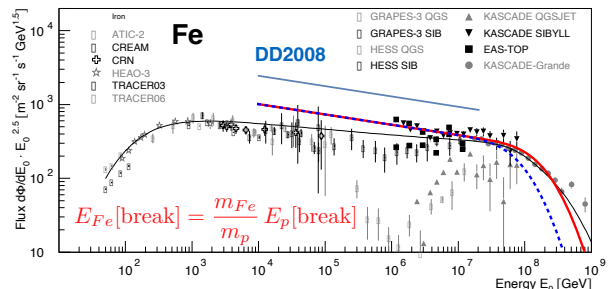


Figure 6: The Fe knee with its predicted break [12].

the observed CR ones are quite extraordinarily different. The enhancement factor $A^{1.75}$ of Eq.(12) snugly serves to predict the CR abundances, and varies from 1 to $\sim 1.22 \times 10^3$ from H to ^{58}Ni . These results follow from the simple CB-model statement that the CR fluxes, as functions of Lorentz factor, are universal.

IV. THE CR SPECTRA ABOVE THEIR KNEES

Data of CR nuclei are sufficient to test Eqs.(2) and (10) for elements up to Fe, as shown in comparing Fig.(6) with Fig.(3). But the data are insufficiently precise to test whether the knee positions scale as A or Z . And they do not reach energies high enough to test the CB-model spectral predictions beyond the knees. To recall them and to clarify a couple of points we reproduce the DD2008 prediction for the galactic flux of protons in Fig.(7).

Two contributions to the galactic proton flux are shown in Fig.(7), excluding the extragalactic contribution, only relevant at very high energies. The ‘elastic’ contribution is the one we have discussed at length. In DD2008 we assumed that a minute fraction of the ISM intercepted by a CB is Fermi-accelerated by the CB’s inner chaotic magnetic field, whose properties we deduced from

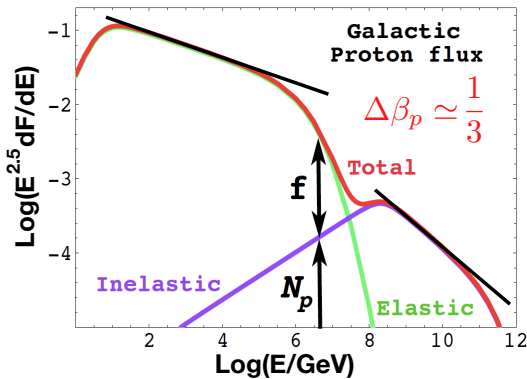


Figure 7: The p spectrum (red), its (black) predicted slopes and its two contributions (green and mauve) [DD2008].

a comparison to the Galaxy’s magnetic fields. When exiting the CB by diffusion these accelerated particles constituted the “inelastic” contribution. In the revamped CB model we assume that a similar process takes place in the “magnetic domain” of a CB. Its shape is also an explicit universal function of γ , Eqs.(37,38) of DD2008. Its predicted slope is $\simeq 1/3$ steeper than that of the elastic contribution, as shown in the figure, that defines “slope” in the sense used here.

The quantity f in Fig.(7) describes the ratio of the two contributions at a given energy. It cannot be fit to the proton data of Fig.(3), but since the CB model correctly predicts the CR abundances of the main elements, an approximate f can be extracted from the all-particle data above the Fe knee. Finally the combined quantity $f \times N_p$ in the figure depends on imprecise priors, such as the rate of Galactic SNe. It was adjusted in DD2008 via the observed proton flux, related to the CR luminosity of the Galaxy, which the CB model accommodates without effort. The ratio of total inelastic to total elastic fluxes is of $\mathcal{O}(10^{-15})$, reacceleration of the initial CRs need not be very efficient.

After three consecutive paragraphs we have been unable to show the full consequences of the prediction described in Fig.(7). But a “surprise” is awaiting in the form of the CR electron flux.

V. THE CR ELECTRON FLUX

Fig.(8) is the electron version of the proton result of Fig.(7). The figures differ in two respects: their energies are scaled by particle mass from a common $dF/d\gamma$ input. And, traveling in the Galaxy, electrons loose energy faster than nuclei; interactions with magnetic fields and the ambient radiation dominate at sufficiently high energy. A detailed analysis in DD2008 and [27] yields the conclusion that, below the knee $\beta_e = \beta_s + 1 \simeq 3.17$. Sharing a common $dF/d\gamma$ with the H spectrum, the e^- spectrum steepens as the knee is crossed by $\Delta\beta_e = \Delta\beta_p \simeq 1/3$. All these predictions are supported by the data in Fig.(8).

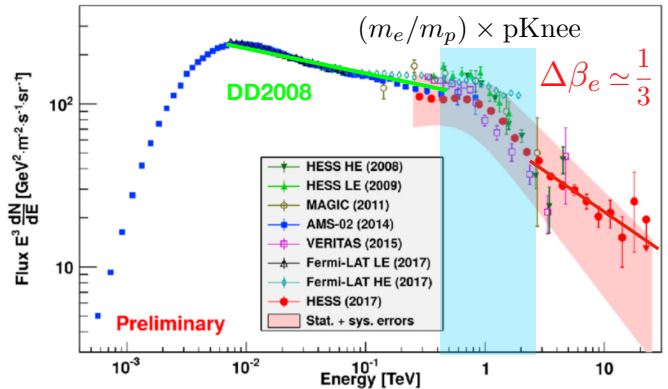


Figure 8: Data compilation [24] and CB-model predictions for high energy CR electrons. The green (red) lines are the predicted slopes below (above) the electron knee region, symbolized by the clear blue domain which, as predicted, occurs at an energy a factor m_e/m_p times that of the proton’s knee.

The knees of CR electron, p, and other nuclear spectra and the peak energy of GRB221009A have a common explanation based on the CBs’ LF distribution extracted from the analysis of their afterglows. This multiple “coincidence” does not seem to be a random one. And the CR break energies scale with mass, definitely not charge.

Notice that in Fig.(8) we have not tried to deal with the low energy data. For them the source spectrum is still a function only of their LF, but at low energies $v/c \neq 1$ plays a role and Eq.(7) is not a good approximation. In spite of this, in DD2008 we showed, for H and He, how the CB-model successfully predicts their observed low-energy spectral shapes, see the Appendix. We have not made a similar analysis of the electron lower-energy data of Fig.(8). The reason is that the task becomes arduous: for such electrons Coulomb scattering and bremsstrahlung energy losses, as well as uncertainties in the confinement time of electrons, play a significant role [DD2008].

VI. THE AMS POSITRON SPECTRUM

The CB-model’s expectation for the spectrum of CR positrons [27] is a subject that, unlike the others discussed here, cannot be summarized in simple terms. Positrons are made in collisions of accelerated nuclei with ambient ones, e.g. pp (or pn) $\rightarrow \pi$ or $K \rightarrow \mu^+ \rightarrow e^+$.

Deriving the e^+ flux requires a lengthy calculation involving many CB-model’s inputs extracted from other observations: the distribution on LFs shown in Fig.(2), the typical CB baryon number (10^{50}), a CBs’ initial expansion velocity in its rest frame (the relativistic speed of sound, $c/\sqrt{3}$) and the SN wind’s surface density (10^{16} g/cm). Other inputs are the number of CR generating SNe in the Galaxy (1/100y), and the number of CBs per SN (10, twice the average number of GRB pulses).

The result of the above calculation [27] is shown in Fig.(9) as the dashed line. Some comments: secondary

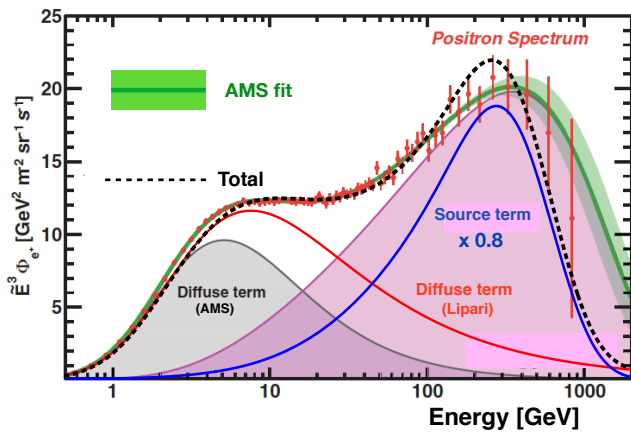


Figure 9: Adopted diffuse term (red) and calculated source term (blue), and their sum (black, dashed).

positrons (the “diffuse term” in AMS parlance) are a not well known “background”, we chose the one labeled Lipari [30]. For esthetics, the “source term” CB model’s prediction has been reduced to 0.8 its calculated value, this fudge factor being much less important than the uncertainties in the inputs⁴.

VII. HIGH-ENERGY NEUTRINOS

The same processes producing positrons produce neutrinos, via decays such as $\pi^\pm \rightarrow \mu^\pm \nu$ and $\mu \rightarrow e \nu \bar{\nu}$. In the line of sight to a GRB, should neutrinos not be observable in coincidence with the GRB proper? Why have they not been detected by IceCube? [31]. The CB-model answer is deceptively simple, see Fig.(10). As remarked in [1] neutrinos produced in proton-induced collisions have transverse momenta of the order of that of their parent mesons, in turn of the order of the mesons’ masses. The consequent neutrino-beam opening angle is much smaller than the one of observable GRB gammas. And the GRB afterglow neutrino flux is negligible [DD2008]. Moreover, to expect a neutrino signal it must be assumed that ambient magnetic fields are weak enough not to deviate the charged parents of neutrinos.

The electrons accelerated by a CB to $\gamma_e \gg \gamma_0[\text{CB}]$ may also scatter ambient light to produce photons of much higher energy than the usual E_γ of $\mathcal{O}(1)$ MeV. But their beam has an aperture $1/\gamma_e \ll 1/\gamma_0[\text{CB}]$, explaining why there are so few GRBs with very high energy photons.

⁴ As shown in [27], Shlomo Dado made a perfect fit to the data by slightly adjusting the input priors. But that is *not* the point. The point is that the “source term” in Fig.(9) is a prediction.

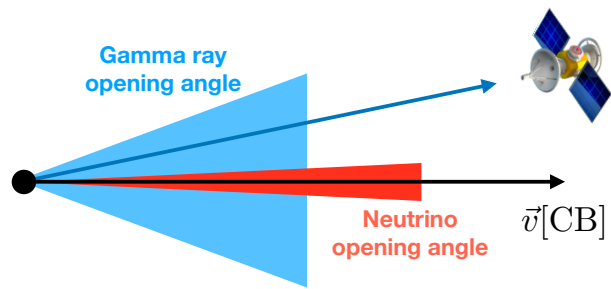


Figure 10: An observed GRB and its missing neutrinos.

VIII. CONCLUSIONS

In the Appendix and in previous articles (e.g. DD2008) we have argued that the CB model provides a satisfactory comprehension of cosmic rays at all energies. Particularly gratifying, in our view, were the analytical results on CR fluxes, including the predictions for the low-energy CR spectra as in Fig.(13) and the very simple explanation of the observed relative CR abundances, as in Fig.(5). These understandings are still “first order” in that we cannot interpret the data in minute detail, see Fig.(4).

The CB model is unsatisfactory in the sense that, though cannonballs have been observed moving superluminally in the plane of the sky [28, 46], we do not have a detailed analytical or numerical understanding of the interactions between CBs and their hypothetical magnetic fields with the ISM. But the current “guesses” –so very successful in the understanding of GRBs [6, 18]– continue to yield good results for CRs as well:

The knee energies of the CR spectra of electrons, H, He and Fe nuclei scale with mass. This is particularly striking when comparing electrons with nuclei, see Figs.(3,6,8). The H knee ends at the energy predicted via the Lorentz factor of GRB221009A, obtained from the CB-model’s interpretation of its peak energy. That peak energy is at the top of the distribution of LFs extracted from the CB-model analysis of GRBs, not of CRs, see Fig.(2). A calculation –with no fit parameters– of the positron spectrum observed by AMS gives a convincing result, see Fig.(9). The non observation of very high energy neutrinos by IceCube has a trivial explanation [1].

One might be tempted to state that, once again, Baron Munchausen’s cannonballs hit their various targets.

Acknowledgment: I am particularly indebted to Shlomo Dado, Arnon Dar and Fabio Truc for discussions and advice. This project has received funding/support from the European Union’s Horizon 2020 research and innovation programme under the Marie Skłodowska-Curie grant agreement No 860881-HIDDeN.

Appendix: The CB model of GRBs and CRs

Jets are emitted by many astrophysical systems, such as Pictor A, shown in Fig. (11). Its active galactic nucleus is discontinuously spitting something that, seen in

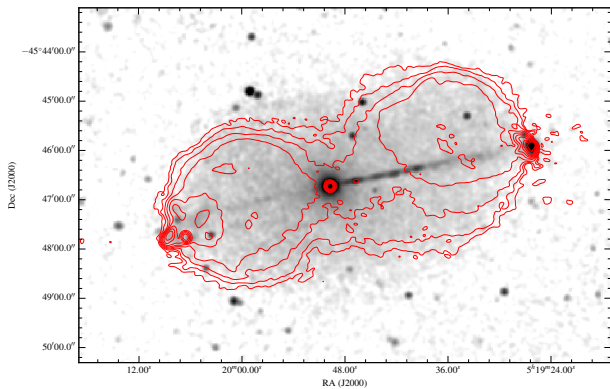


Figure 11: The quasar Pictor A. A superposition of an X-ray image and the (red) contours of the radio emission [32].

X-rays, does not appear to expand sideways before it stops and blows up, having by then travelled almost 10^6 light years. Many such systems have been observed. The Lorentz factors of their ejecta are of $\mathcal{O}(10)$. The mechanism responsible for the ejections, due to episodes of violent accretion into a black hole, is not well understood.

The radio signal in Fig. (11) is the synchrotron radiation of ‘cosmic-ray’ electrons [32]. Electrons and nuclei were scattered by the CBs of Pictor A, which encountered them at rest in the intergalactic medium, kicking them up to high energies. Thereafter, these particles diffuse in the ambient magnetic fields—that they contribute to generate—and the electrons radiate.

In our galaxy there are ‘micro-quasars’, whose central black hole’s mass is a few M_{\odot} . The best studied [33] is GRS 1915+105. A-periodically it emits two oppositely directed *cannonballs*, traveling at $v \sim 0.92c$. When this happens, the continuous X-ray emissions—attributed to an unstable accretion disk—temporarily decrease. Atomic lines of many elements have been seen in the CBs of μ -quasar SS 433 [34]. Thus these ejecta are made of ordinary matter.

The ‘cannon’ of the CB model is analogous to the ones of quasars and μ -quasars, though with larger LFs. In the core-collapse responsible for a stripped-envelope SNic event, due to the parent star’s rotation, an accretion disk is produced around the newly-born compact object, by stellar material originally close to the imploding core, or by more distant matter falling back after the shock’s passage. A CB made of *ordinary-matter plasma* is emitted, as in μ -quasars, when part of the accretion disk falls onto the compact object. *Long-duration* GRBs, XRFs and *non-solar* CRs are produced by these jetted CBs.

A summary of the CB model is given in Fig. 12. The ‘inverse’ Compton scattering (ICS) of light by electrons within a CB produces a highly forward-collimated beam of higher-energy photons. The target light is in a temporary reservoir: the *glory*, an “echo” (or ambient) light from the SN, permeating the “wind-fed” circumburst density profile, previously ionized by the early UV flash accompanying a SN explosion and/or by the enhanced UV emission that precedes it. To agree with observations, CBs must have baryon numbers N_B of $\mathcal{O}(10^{50})$,

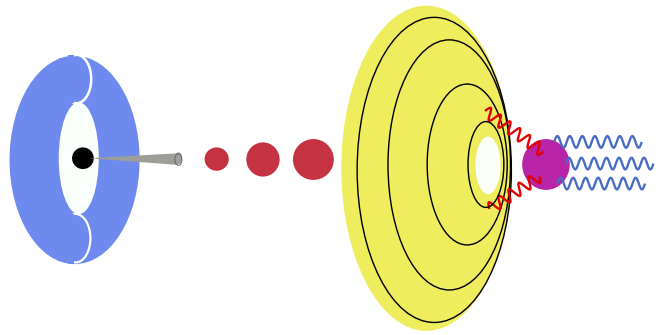


Figure 12: An ‘artist’s view’ (not to scale) of the CB model of long-duration GRBs. A core-collapse SN results in a compact object and a fast-rotating torus of non-ejected fallen-back material. Matter (not shown) abruptly accreting into the central object produces a narrowly collimated beam of CBs, of which only some of the ‘northern’ ones are depicted. As these CBs move through the ‘ambient light’ surrounding the star, they Compton up-scatter its photons to GRB energies.

$\sim 1/2$ the mass of Mercury, a miserable $\sim 10^{-7} M_{\odot}$.

The simple kinematics describing a beam of GRB or XRF photons—viewed at different angles—suffice to predict all observed correlations between pairs of prompt observables, e.g. photon fluence, energy fluence, peak intensity and luminosity, photon energy at peak intensity or luminosity, and pulse duration. The correlations are tightly obeyed, indicating that observable GRBs are moderately standard candles—with “absolute” properties varying over a couple of orders of magnitude—while the observer’s angle makes their apparent properties vary over very many orders of magnitude [35]. Double and triple correlations of GRB observables and the “break time” of their afterglows agree with the CB model [36]. The shapes of GRB pulses and their spectrum are also neatly explained by ICS of glory light [6].

In its journey through its host galaxy, a CB encounters the constituents of the ISM, previously ionized by the GRB’s γ -rays. The CB itself or, more likely, the collision of its magnetic field with the ISM electrons and nuclei results in CRs. GRBs and XRFs have long-lasting ‘afterglows’ (AGs). The CB model accounts for them as synchrotron radiation from the ambient electrons swept in by the CBs, predicting the correct fluencies, AG light curves and spectra [38, 39].

The obstacles still separating the CB model from a complete theory of CRs and GRBs are the theoretical understanding of the CBs’ ejection mechanism in SN explosions and of the precise way in which a CB’s assumed magnetic field interacts with the ISM. Otherwise the CB model describes all known properties of GRBs and XRFs. But, perhaps more significantly, the model also resulted in remarkable predictions:

The SN-GRB association

GRB980425 was ‘associated’ with SN1998bw: within directional errors and within a timing uncertainty of ~ 1 day, they coincided. The luminosity of a 1998bw-like SN peaks at $\sim 15(1+z)$ days. *Iff* one has a predictive theory

of AGs, one may test whether GRBs are associated with ‘standard torch’ SNe, akin to SN1998bw, ‘transported’ to the GRBs’ redshifts. The test was already conclusive (to us) in 2001 [38]. One could even *foretell the date* in which a GRB’s SN would be discovered. For example, GRB030329 was so ‘near’ ($z = 0.168$) that we could not resist posting such a daring prediction [40] during the first few days of AG observations. The spectrum of this SN snugly coincided with that of SN1998bw. The prediction of where and when a SN would be seen was shortened from thousands of years to just one night.

The AG light curves

Swift has established a “canonical behaviour” of the X-ray and optical AGs of a large fraction of GRBs. The X-ray fluence decreases very fast from a ‘prompt’ maximum. It subsequently turns into a ‘plateau’. After a time of $\mathcal{O}(1d)$, the fluence bends (has an achromatic ‘break’, in the usual parlance) and steepens to a power-decline. Although all this was considered a surprise, it was not [41]. Even GRB980425, the first to be clearly associated with a SN, sketched a canonical X-ray light curve, with what we called a ‘plateau’ [38]. Scores of X-ray and optical AGs are correctly described by the CB model [38, 39].

The (apparent!) superluminal motion

One may state that to support the CB model, cannonballs ought to be clearly “seen”, as in the μ -quasar XTE J1550-564 [42]. Only in two SN explosions that took place close enough the CBs were in practice observable. One case was SN1987A, in the LMC, whose approaching and receding CBs were photographed [43]. The other was SN2003dh, associated with GRB030329, at $z = 0.1685$. In the CB model interpretation, its two approaching CBs were first ‘seen’, and fit, as the two-peak GRB and the two-shoulder AG. This allowed us to estimate [44] the time-varying angle of their apparent superluminal motion [45] in the sky. Two sources or ‘components’ were seen in radio observations at a date coincident with an optical AG re-brightening. The data agree with the predictions including the inter-CB separation [44]⁵. The observers claimed the contrary, though the evidence for the weaker ‘second component’ is $> 20\sigma$, and they [46] closed the issue by stating in their abstract: “The presence of this component is not expected from the standard model”⁶.

GRB GW170817/SHB170817A is not a long, but a short GRB: a neutron star merger and gravitational-wave source. In its radio afterglow, a CB was observed with an⁵ The size of a CB is small enough for its radio image to scintillate, arguably more than observed [46]. But the ISM electrons a CB scatters, synchrotron-radiating in the ambient magnetic field, significantly contribute at radio frequencies, blurring the CBs’ radio image [44]. Also, during the time of a radio observa-

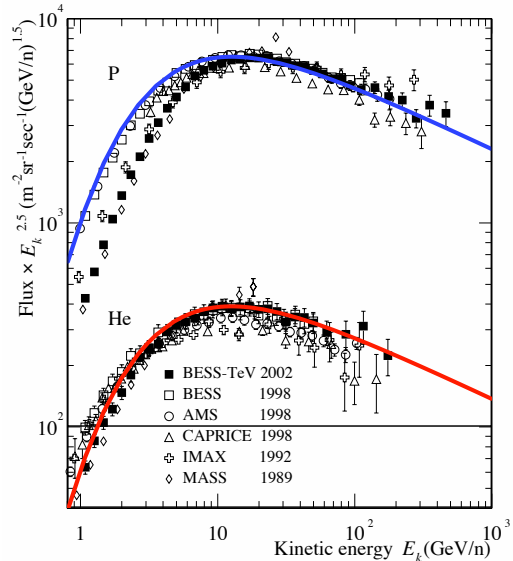


Figure 13: The very low energy fluxes of protons and α particles at various times in a solar cycle. The 1998 data are close to solar-minimum time.

overwhelming statistical significance ($> 17\sigma$) and traveling in the plane of the sky, as expected, at an apparent superluminal velocity $V_{app} \sim 4c$ [28].

The Low-Energy CRs

The universal flux of Eq.(10) is a $\gamma \gg 1$ approximation of a slightly more complicated expression, Eq.(33) of DD2008, applicable for all CR energies. For p and He fluxes, the result is shown in Fig.(13). A remarkable point is that in the figure only the absolute flux normalizations –and no other parameters– have been adjusted.

The GRB’s γ -ray polarization

Earliest but not least [48, 49]. Let a CB launched with a LF γ_0 be seen at an angle θ from its jetted direction. The observed γ -rays, having been Compton up-scattered, have a polarization $\Pi \approx 2\gamma_0^2 \theta^2 / (1 + \gamma_0^4 \theta^4)$. This vanishes on axis, is nearly 100% for the most probable viewing angle ($\theta \sim 1/\gamma_0$) and $> 47\%$ for $2/\gamma_0 > \theta > 1/(2\gamma_0)$. All measured GRB polarizations [50] are $> 47\%$, but two, 930131 and 100826A, whose polarizations are also incompatible with $\Pi = 0$, the expectation for synchrotron radiation of electrons in a non-structured magnetic field.

tion the CBs move, obliterating the scintillations [47].

⁶ Imagine the reaction to a similar challenge in cosmology or particle physics, realms where there are “standard” models strongly supported by data and successful predictions.

[1] Shlomo Dado and Arnon Dar, Journal of Modern Physics, **15**, 125 (2024).

[2] [https://www.etsy.com/listing/1219140266/printable-](https://www.etsy.com/listing/1219140266/printable-wall-art-baron-munchausen)

wall-art-baron-munchausen

[3] Key ideas underlying the CB model were adopted from: N. J. Shaviv, A. Dar, ApJ, **447**, 863 (1995), arXiv:astro-

- ph/9407039.
- A. Dar, ApJ, **500**, L93 (1998), arXiv:astro-ph/9709231.
- A. Dar A&AS, **138**, 505 (1999), arXiv:astro-ph/9902017.
- A. Dar, R. Plaga, A&A **349**, 259 (1999), arXiv:astro-ph/9902138.
- A. Dar, A. De Rújula, 2000, arXiv:astro-ph/0012227.
- S. Dado, A. Dar, A. De Rújula, A&A, **388**, 1079D (2002), arXiv:astro-ph/0107367.
- [4] J. Goodman, A. Dar, S. Nussinov, ApJ, **314**, L7 (1987).
- [5] M. J. Rees, P. Meszaros, MNRAS, **25**, 29 (1992).
- [6] A. Dar, A. De Rújula, Phys. Rep. **405**, 203 (2004), arXiv:astro-ph/0308248.
- [7] A. Dar and A. De Rújula, Phys. Rept. **466**, 179 (2008), hep-ph/0606199.
- [8] Bon-Chul Koo et al. The Astrophysical Journal, Volume 905, Number 1.
- [9] D. Frederiks et al. The Astrophysical Journal Letters, **949**, L7 (2023).
- [10] A. Dar & A. De Rújula, arXiv:astro-ph/0012227, S. Dado, A. Dar and A. De Rújula, Astrophys. J. **663**, 400 (2007).
- [11] L. Amati, F. Frontera, M. Tavani, et al., A&A, **390**, 81 (2002), arXiv:astro-ph/0205230.
- [12] A. De Rújula, Phys. Letts. B 790C, **444** (2019), arXiv:1802.06626.
- [13] L.O. Silva & al., Astrophys. J. **596**, L121 (2003). T. Haugboelle & al., Procs. 22nd Texas Symp. on Relativistic Astroph. (2004), astro-ph/0503332v1. Jacob Trier Frederiksen & al., Astroph. J. Letters **722**, L114 (2010), arX1003.1140v4.
- [14] Troy A. Porter, Gudlaugur Johannesson & Igor V. Moskalenko, The Astrophysical Journal Supplement **262**, 30 (2022), arXiv:2112.12745
- [15] A. De Rújula, Howard Georgi & S.L. Glashow, Phys.Rev. D12 147 (1975).
- [16] A. De Rújula, Int. J. of Modern Physics A **34**, No. 32, 1930015 (2019).
- [17] P.A. Zyla et al. (Particle Data Group), Prog. Theor. Exp. Phys. 2020, 083C01 (2020) and 2022 update.
- [18] S. Dado, A. Dar and A. De Rújula, Special issue on GRBs, MDPI journal “Universe”, <https://www.mdpi.com/2218-1997/8/7/350/pdf>, arXiv:2204.04128.
- [19] A.M Hillas, astro-ph/0607109v2.
- [20] Arnon Dar & A. De Rújula, arXiv:hep-ph/0611369
- [21] For AMS results, see, e.g., Phys. Rep. **894**, 1 (2021), <https://indico.cern.ch/event/1275785/>
- [22] See, e.g. S.P. Swordy & al., Astrophys. J. **349**, 625 (1990).
- [23] Zhen Cao & al. Phys. Rev. Lett. **132**, 131002.
- [24] www.mpi-hd.mpg.de/HESS/pages/home/som/2017/09/
- [25] B. Wiebel-Sooth, P. Bierman & H. Meyer, Astron. & Astrophys. **330**, 37 (1998).
- [26] N. Grevesse & A.J. Sauval, 1998, Sp. Sci. Rev. **85**, 161 (1998); N. Grevesse & A.J. Sauval, Adv. Sp. Res. **30**, 3, (2002).
- [27] A. De Rújula, arXiv:1909.01277.
- [28] A. De Rújula, Il Nuovo Cimento C, **1** (2023), arXiv:2204.07418.
- [29] G. B. Taylor, et al., ApJ, **609**, L1 (2004), arXiv:astro-ph/0405300v1
- [30] P. Lipari, arXiv:1810.03195v1.
- [31] R. Abbasi, et al., arXiv:2205.11410.
- [32] M. J. Hardcastle et al. MNRAS, **455**, 3526 (2016).
- [33] I.F. Mirabel & L.F. Rodriguez, Annu. Rev. Astron. Astrophys. **37**, 409 (1999).
- [34] S.S. Eikenberry & al., Astrophys. J. **561**, 1027 (2001); D.R. Gies & al., Astrophys. J. **566**, 1069 (2001); M.G. Watson & al., Mon. Not. Roy. Astron. Soc. **222**, 261 (1986); T. Kotani & al., Publ. Astron. Soc. Jap. **48**, 619 (1996); H.L. Marshall, C.R. Canizares & N.S. Schulz, Astrophys. J. **564**, 941 (2002); S. Migliari, R. Fender & M. Méndez, Science **297**, 1673 (2002); M. Namiki & al., Publ. Astron. Soc. Jap. **55**, 1 (2003).
- [35] A. Dar & A. De Rújula, arXiv:astro-ph/0012227; S. Dado, A. Dar & A. De Rújula, Astroph. J. **663**, 400, (2007), Astroph. J. **693**, 311, (2009), Astroph. J. **696**, 994, (2009).
- [36] S. Dado & A. Dar, Astroph. J. **755**, 16, (2013).
- [37] J.K. Frederiksen & al., Astrophys. J. **608**, L13 (2004).
- [38] S. Dado, A. Dar & A. De Rújula, Astron. & Astrophys. **388**, 1079 (2002).
- [39] S. Dado & A. Dar, Phys. Rev. **D94**, 063007 (2016).
- [40] S. Dado, A. Dar & A. De Rújula, Astroph. J. **594**, L89 (2003).
- [41] S. Dado, A. Dar & A. De Rújula, Astroph. J. **646**, L21 (2006).
- [42] S. Corbel & al., New Astron. Rev. **47**, 477 (2003).
- [43] P. Nisenson & C. Papaliolios, Astrophys. J. **518**, L29, (1999).
- [44] S. Dado, A. Dar & A. De Rújula, arXiv:astro-ph/0402374, 0406325
- [45] P. Courdec, Annales d’Astrophysique **2**, 271 (1939). M. J. Rees, Nature, **211**, 468 (1966).
- [46] G.B. Taylor & al. Astrophys. J. **609**, L1, (2004).
- [47] S. Dado, A. Dar & A. De Rújula. arXiv:1712.09970.
- [48] N. J. Shaviv and A. Dar, ApJ **447**, 863 (1995).
- [49] S. Dado, A. Dar & A. De Rújula, arXiv:astro-ph/0403015; arXiv:astro-ph/0701294 and in Proceedings of the Vulcano Workshop on Frontiere Objects in Astrophysics, May 21-27, 2006, Vulcano Italy.
- [50] GRB 021206. W. Coburn & S. E. Boggs, Nature **423**, 415 (2003). GRBs 930131, 960924. D. R. Willis, & al. 2005, A&A, **439**, 245 (2005). GRB 041219A: E. Kalemci & al. ApJS, **169**, 75 (2007). GRB 041219A: McGlynn & al. A&A, **466**, 895 (2007). GRB 100826A: Yonetoku & al. ApJ, **743**, L30 (2011). GRBs 110301A and 110721A: Yonetoku & al. ApJ, **758**, L1 (2012). GRB 061122: Gotz & al. MNRAS **431**, 3550, (2013). GRB 140206A: Gotz & al. MNRAS **444**, 2776 (2014).